

This is an Open Access document downloaded from ORCA, Cardiff University's institutional repository:<https://orca.cardiff.ac.uk/id/eprint/101627/>

This is the author's version of a work that was submitted to / accepted for publication.

Citation for final published version:

Preedy, Emily Callard, Perni, Stefano and Prokopovich, Polina 2017. Cobalt and titanium nanoparticles influence on mesenchymal stem cell elasticity and turgidity. *Colloids and Surfaces B: Biointerfaces* 157 , pp. 146-156. 10.1016/j.colsurfb.2017.05.019

Publishers page: <http://dx.doi.org/10.1016/j.colsurfb.2017.05.019>

Please note:

Changes made as a result of publishing processes such as copy-editing, formatting and page numbers may not be reflected in this version. For the definitive version of this publication, please refer to the published source. You are advised to consult the publisher's version if you wish to cite this paper.

This version is being made available in accordance with publisher policies. See <http://orca.cf.ac.uk/policies.html> for usage policies. Copyright and moral rights for publications made available in ORCA are retained by the copyright holders.



Cobalt and Titanium Nanoparticles Influence on Mesenchymal Stem Cell Elasticity and Turgidity

by

Emily Callard Preedy¹, Stefano Perni¹, Polina Prokopovich^{1,*}

¹ School of Pharmacy and Pharmaceutical Sciences, Cardiff University, Cardiff, UK

word count abstract: 148

complete manuscript word count: 4788

number of references: 50

number of figures/tables: 8/0

* Corresponding author:

Dr. Polina Prokopovich e-mail: prokopovichp@cardiff.ac.uk

School of Pharmacy and Pharmaceutical Sciences

Cardiff University

Redwood Building, King Edward VII Avenue

Cardiff, UK

CF10 3NB

Tel: +44 (0)29 208 75820

Fax: +44 (0)29 208 74149

Abstract

Bone cells are damaged by wear particles originating from total joint replacement implants. We investigated Mesenchymal stem cells (MSCs) nanomechanical properties when exposed to cobalt and titanium nanoparticles (resembling wear debris) of different sizes for up to 3 days using AFM nanoindentation; along with flow-cytometry and MTT assay. The results demonstrated that cells exposed to increasing concentrations of nanoparticles had a lower value of elasticity and spring constant without significant effect on cell metabolic activity and viability but some morphological alteration (blebbing). Cobalt induced greater effect than titanium and this is consistent with the general knowledge of cyto-compatibility of the later.

This work demonstrates for the first time that metal nanoparticles do not only influence MSCs enzyme activity but also cell structure; however, they do not result in full membrane damage. Furthermore, the mechanical changes are concentration and particles composition dependent but little influenced by the particle size.

Keywords: Mesenchimal Stem Cells, wear particles, nanomechanical properties, AFM, Titanium nanoparticles, Cobalt nanoparticles

1 Background

Cells are sensitive to forces, stiffness and adhesion [1] such as the stresses (forces) and strains (deformation) of their environment [1],[2]; therefore, cells can respond to internal as well as external forces, detecting the mechanics of interacting substrates will generate internal forces which depend on the mechanical properties of the cell [3]. These mechanical properties of cells have been of interest [2],[4] in the understanding of certain pathological disorders including cancer, osteoporosis, atherosclerosis, and osteoarthritis [3]. As these stresses and strains exerted on cells can generate signals similar to chemical stimuli which initiates cell growth, promoting cell survival and differentiation, as well as apoptosis [1].

Articulating surfaces of medical implants, resulting from total joint replacement surgeries, generate a large number of particles as a result of wear process over time [5]. Damage from wear can directly affect the implanted device causing loss of tolerance, friction and therefore the expected longevity of the device is minimised [6]. wear particles also initiate an immune response inducing aseptic loosening, and osteolysis [6]-[8]. The cellular mechanism of the response to wear particles involves macrophages, monocytes, osteoblasts, and osteoclasts cells [9]-[10]. The issues highlighted have an inherent affect disrupting the normal bone remodelling process and implant acceptance [11],[12]. Disruptions commonly occur due to the uptake of nano-sized metal particles to surrounding cells which are biologically active causing greater inflammation, DNA and chromosome damage, cytokine release and cytotoxicity in cells than their micro-sized counterparts [8],[13]-[15]; and has been recognised as a current problem in orthopaedic implants as metal-on-polyethylene and metal-on-metal (MoM) implants generate large numbers of particles (such as cobalt chromium, titanium, and polyethylene) [12],[16],[17].

Osteoprogenitor cells have been implicated as another target in particle-mediated osteolysis [18]-[22]. Multipotent mesenchymal stem cells (MSCs) in trabecular bone [23]-[24] and adjacent to implants have osteoprogenitor activities and are critical contributors to maintaining osseous tissue integrity. Perturbation of MSC osteogenic activity may thus affect bony ingrowth and interface stability, leading to increased risk of loosening.

While many studies have focused on the effect of particles on macrophages [25] or osteoprogenitor cells [18]-[19], in terms of reduced osteogenic differentiation and

proliferation and enhanced apoptosis, differential and combined effects of cell mechanical properties after exposure to wear particles have not been studied. The cell cytoskeleton, to a large extent, is responsible for the structural and mechanical integrity of cells and takes an active role in signalling pathways (i.e. mechanotransduction). Thus, any changes in the cell structure will result in changes to the mechanical properties of the cell and consequently its functionality. Hence, the ability to measure mechanical properties of cells at different levels, in particular the nano-level, might be considered a powerful method to assess cell and tissue functionality. Recently, there has been a significant increase in number of studies investigating mechanical properties of cell/tissue [26],[27]. Investigations of the impact of diverse physiological conditions on the mechanical properties of various cells, expressed mainly as stiffness, and quantified by the Young's modulus have given us a new understanding of the cell; leading to discoveries of complex pathways that govern cell responses and functionality [28]-[30].

In this study, we hypothesised that exposure to cobalt and titanium nanoparticles will modify MSC cells nanomechanical and adhesive properties. Therefore, the aim of this study was to directly quantify the elasticity, turgidity and adhesiveness of MSCs after exposure for different periods of time to cobalt and titanium nanoparticles of various compositions, sizes and charges employing AFM. The findings from cell nanomechanical and adhesive properties also were complemented by cells viability and metabolic activity studies.

2 Methods

2.1 Cell Culture

28 days old, male Wistar rats were obtained from the colony maintained by Charles River European Suppliers (Charles River UK Ltd., Kent, UK). The animals were housed with free access to water and were maintained with treatment and care protocols conformed to UK Animals (Scientific Procedures) Act 1986, accordance to the European Convention for the Protection of Vertebrate Animals Used for Experimental and Other Scientific Purposes (Strasbourg, Council of Europe). Rats were sacrificed by schedule 1 procedures of culling and harvest of tissue by a trained and licenced technician. The appropriate procedures and measures were employed in all cases to minimize animal suffering, adverse effects and any

pain, suffering, distress or lasting harm according to the Home Office Code of Practice “Humane killing of animals under Schedule 1 to the Animals for Scientific Procedures act. Bone marrow stem cells were isolated from rat femur and humerus, using plastic adherence [31], followed by fibronectin adherence techniques [32]. After 7 days, merged colonies were expanded (passage 0). The cells were routinely cultured in α -MEM (Life Technologies), supplemented with 20% (v/v) FBS, 1% (v/v) of solution penicillin (5000 U/mL) and streptomycin (5000 mg/L) (Gibco Invitrogen) and 1% (v/v) of L-ascorbic acid 2-phosphate solution at 50 mg/ml (Sigma, UK). Accutase (Gibco Invitrogen) was used when cells were 70% confluent in order to passage and count. The cells were maintained at 37° C in a humidified atmosphere containing 5% CO₂.

For atomic force microscopy experiments, cells were seeded in 24-well plates at a density of 6000 cells per well and cultured for 24 hours on sterilised polystyrene slides placed inside the well before exposure to nanoparticles. For each type of nanoparticles a stock solution of the nanoparticles suspended in culture media was prepared at 5 mg/ml and appropriate amount was added to each well to reach final concentrations of 5; 12.5; 25 and 50 μ g/ml and incubated from 24h up to 3 days. Control samples consisting of cells not exposed to nanoparticles and cultured in the same conditions were used for comparison with treated cells.

2.2 Nanoparticles

Commercially available nanoparticles were obtained of various sizes and compositions from Sigma Aldrich, UK. For cobalt (Co) nanoparticles (NPs), two samples were employed:

- Co elemental, 30nm diameter (referred as ‘Co 30nm’ throughout the text);
- Co (II,III) oxide, 50nm diameter (referred as ‘Co 50nm’ throughout the text).

Three samples of titanium (Ti) were employed:

- Ti elemental, 30nm diameter;
- Ti (IV) oxide anatase, 25nm diameter; and
- mixture of Ti (IV) oxide rutile and anatase, 100nm diameter

They are referred to as 'Ti 30nm', 'Ti 25nm' and 'Ti 100nm', respectively, throughout the text.

All nanoparticles were weighed and suspended in α -MEM medium to make a stock suspension of nanoparticles of 5mg/ml. From this stock solution, a number of nanoparticles concentrations (5 μ g/ml; 12.5 μ g/ml; 25 μ g/ml and 50 μ g/ml) were prepared.

2.3 Metabolic activity assay

MTT assay was used to determine the effects of the metal nanoparticles on MSCs metabolic activity. After the chosen exposure to nanoparticles, the media was replaced with phenol red-free medium and 80 μ l of MTT stock solution (5mg/ml) was added to each well and incubated at 37°C in humidified atmosphere containing 5% CO₂ for 2 hour. The metabolised formazan was re-suspended with 800 μ l of dimethyl-sulfoxide (DMSO). 200 μ l were transferred to a 96-well plate absorbance at 560nm was read using a spectrophotometer (ELISA Reader Labtech LT-5000MS). All experiments were performed in triplicates with each nanoparticles concentration as well as a control sample of cell suspension not exposed to nanoparticles.

2.4 Flow-Cytometry

Viability of MSC after exposure to nanoparticles was determined using LIVE/DEAD® Viability/Cytotoxicity Kit, for mammalian cells (Life Technology, UK) through flow-cytometry. Two fluorescent stains were used: calcein-AM (Ex 480nm / Em 520nm) and ethidium homodimer-1 (Ex 520nm / Em 615nm); the former returns green fluorescence when interacting with living cells; whilst the later binds to nucleic acids with red fluorescence only through the compromised membrane as it is cell impermeant.

BD FACSVerse™ was used; after the chosen exposure time elapsed; cells were washed with PBS and trypsinised then re-suspended in sterile PBS. 1 ml of this cell suspension was placed into Eppendorf and centrifuged at 24 °C, for 5 minutes at 1800 rpm (363 g). The supernatant was removed and the pellet of cells in the Eppendorf was resuspended in PBS. 7 μ l of both dye solutions, prepared as manufactured recommended were added; then cells were vortexed and left for at least 15 minutes in the dark; after 15 minutes the samples were again centrifuged. Post this centrifugation, the supernatant was removed and the cells re-

suspended in PBS, all samples were transferred to FACS tubes prior to sampling. Data collected were then analysed using FlowJo software (LLC, Data Analysis Software, Oregon, USA) to generate four quadrant plots.

2.5 Fluorescent Microscopy

MSCs were stained with Fluorescein Diacetate (FDA; 4 mg/ml in PBS) and Propidium Iodide (PI; 40 mg/ml in PBS), after for 3 min in the dark they were rinsed in fresh PBS. Images of the cells were taken with an Epifluorescent microscope (Leica DM, IRB) using a 10X objective. Cell viability assessment was possible as FDA stained viable cells in green and PI stained non-viable cells in red. Cell nanomechanical properties measurements

All AFM force measurements were conducted in an open liquid cell as described in [33], using PBS as the aqueous phase. A triangular tipless cantilevers (Bruker, UK) with a nominal spring constants ($K_{cantilever}$) of 0.1 N/m was used; the actual spring constant of the AFM cantilever was determined using the Sader method [34],[35]. Borosilicate glass beads (10 μ m in diameter) were glued onto the cantilever and served as cell indentors. In order to prevent indentations depth greater than 400-500 nm, the maximum applied load was set, after preliminary tests, to 1 nN or 2 nN depending on the samples. At least 15 cells were analysed for each sample, at each concentration and at each time point (24, 48, and 72 hours). Cells were first located and then at least 20 approaching and retracting z-piezo coordinates vs. deflection curves were extracted from randomly selected points on the surface of each cell avoiding the peri-nuclear region. Experiments were performed in triplicates.

2.5.1 Cell elasticity and turgidity determination

The approaching part (trace) of the AFM curves was used to calculate the nanomechanical properties of the cells. The Young modulus of the cell surface location under investigation was determined fitting the Hertz model (Eq. 1) to the first part of the indentation vs. force curve after contact between AFM tip and cell surface.

$$F = \frac{4}{3} \frac{E}{(1-\nu^2)} \sqrt{R} \delta^{3/2} \quad (1)$$

Where:

$F =$ force recorded by AFM

$E =$ Young modulus

$R =$ radius of the spherical indenter ($5 \mu\text{m}$)

$\nu =$ Poisson ratio (assumed 0.5)

$\delta =$ indentation depth

The spring constant of the cell surface in the location probed was determined through the slope of the curve after the Hertzian regime according to:

$$F = k_b \delta \quad (2)$$

Where:

$F =$ force recorded by AFM

$K_b =$ spring constant of the cell

$\delta =$ indentation depth

Both models require the determination of the separation between cell surface and AFM tip (δ), this was calculated from the coordinates (z-piezo) of the trace curve assuming that the point of contact corresponded to the local minimum of force; from this:

$$\delta = |z - z_0| - d_{cant} \quad (3)$$

Where:

$z_0 =$ z-piezo value of the minimum of the trace curve

$z =$ z-piezo value of the trace curve

$d_{cant} =$ cantilever deflection

$\delta =$ indentation depth

and

$$F = K_{Cantilever} d_{cant} \quad (4)$$

Both Eq. 1 and 2 were fitted to the data using the least squares method through an in-house written FORTRAN code.

Overall surface heterogeneity of nanomechanical properties was studied through the spatial distribution of E and P_0 .

2.5.2 Cell Adhesion force

The adhesion forces between a cell and AFM tip were determined as the minimum value of the retracting (retrace) part of the AFM curve.

2.6 Cell metal uptake quantification

Quantification of the cells uptake of the metal nanoparticles was gained by using inductively coupled plasma-mass spectroscopy (ICP-MS). All media was removed from each well, cells were washed twice with sterile PBS, and 500 μ l of sub-boiled nitric acid (50 % v/v) was added to each well. The 24-well plate was then placed in an incubator for 24 hours at 60°C in order to digest the cells. After 24 hours in the incubator, from each well 400 μ l of the solution was transferred into a 15 ml polypropylene tube and filled to a total volume of 8 ml with Milli-Q water. ICP-MS analysis was carried out at sample rate of 1.5ml/min and at characteristic wavelengths of 288.616 nm and 334.940 nm for cobalt and titanium ion determination respectively on the Optima 2100DV OES (Perkin Elmer, Waltham, MA, USA) against the Primar 28 element standard.

All experiments were performed independently at least 3 times, and each experiment comprised 3 parallel samples. Results are given as mean \pm standard deviation.

2.7 Statistical analysis

Comparison of the effect of Ti and Co nanoparticles on mechanical properties of MSCs was performed through ANOVA test followed *post hoc* by Tukey's test individual pairs of data

sets ($p < 0.05$). Adhesion forces were compared using the Kruskal-Wallis test followed *post hoc* with a Dunn's test for individual pairs of data sets. Statistical analysis was performed using SPSS.

3 Results

3.1 Metabolic activity

MSC metabolic activity, as assessed through MTT, declined with time over a period of 72 hours regardless of nanoparticles exposure as the control metabolic activity also reduced with time (Figure 1).

After 24 hours exposure (Figure 1) at each of the concentration tested, Ti 100nm had the greatest impact on the metabolic activity at each concentrations tested ($p < 0.05$) whilst Ti 30nm and Ti 25nm returned a lower metabolic activity for concentration greater than 12.5 $\mu\text{g/ml}$; furthermore the effect was monotonically growing with growing concentrations. However, after 48hours Ti 25nm demonstrates a significant impact on the overall metabolic activity. The effect was also concentration dependent, but at the lowest concentration tested, non statistically significant differences were detected compared to MSCs not exposed to nanoparticles ($p > 0.05$). Titanium nanoparticles decreased the cell metabolic activity at concentrations greater than 12.5 $\mu\text{g/ml}$ (Figure 1) irrespectively of the particles size. Only after 48 hours of exposure the size had an impact on cells viability; the smallest nanoparticles gave the lowest viability and the largest (100 nm) are the highest. After 72 hours in contact with Ti nanoparticles, MSCs had the same metabolic activity as the cells not exposed to such particles ($p > 0.05$).

Elemental Co had a lower value of viability compared to the bigger Co 50nm particles after exposure for 24 hour at concentrations higher than 5 $\mu\text{g/ml}$ ($p < 0.05$) (Figure 1). Moreover, the concentration of both types of nanoparticles did not influence the metabolic activity over the range tested ($p > 0.05$). The same was observed after 48 hours for Co 30nm and for Co 50nm.

Similar to case with Ti nanoparticles, MSCs had the same metabolic activity, as the cells not exposed to Co nanoparticles after contact for 72 hours regardless of the size, concentration and composition ($p>0.05$).

3.2 Cell structural integrity

Evidence that the cell membrane integrity was not compromised by any type (composition and size) of nanoparticles, regardless of the concentration, could be seen from the results of flowcytometry (Figure 2). These demonstrate that the cell population was almost entirely comprised by cells exhibiting high green fluorescence, related to calcein AM uptake, and low red fluorescence, related to ethidium homodimer-1, at any exposure time for any of the particles tested.

Epifluorescent microscopy images (Figure 3) confirmed that MSC population was almost entirely viable after exposure to Co nanoparticles; images also suggested alterations in the structure of MSCs after exposure to Co nanoparticles in comparison with control samples.

3.3 Nanomechanical properties

Cell elasticity and spring constant were estimated through modelling the two parts of the AFM indentation curve (Figure 4). The initial part of the indentation followed the Hertz model, whilst with greater indentation the force vs. indentation curve appeared linear.

MSC nanomechanical properties (elasticity and spring constant) were normally distributed. The elasticity of MSCs not exposed to nanoparticles (Figure 5) after 24 hours was about 20 kPa and decreased to about 15 kPa after 2 days and about 10 kPa after 3 days. MSCs generally exhibited a decrease in elasticity (E) as the concentration of titanium nanoparticles increased, even the smallest concentration of 5 $\mu\text{g/ml}$ had a significant effect on the cell elasticity (Figure 5) after 24 hours of exposure regardless of the titanium nanoparticle type. Moreover, no difference was recorded at concentration greater than 25 $\mu\text{g/ml}$ ($p>0.05$). With increasing contact time (48 hours) only Ti 100nm reduced the cell elasticity compared to MSC unexposed to particles and after 72 hours no difference was recorded in cell elasticity between control samples and exposed to any of the Titanium nanoparticles regardless of the concentration ($p>0.05$).

The size and chemical composition (elemental or oxide) of Co nanoparticles did impact on the cell elasticity (Figure 6) after 24 hours of exposure with Co 30nm returning lower values of E at concentrations up to 12.5 $\mu\text{g}/\text{ml}$. Whilst Co 50 nm had a concentration dependent reduction of the cell elasticity. With increasing exposure time to 48 hour and 72 hours, to both types of Cobalt nanoparticles no difference in cell elasticity was detected against MSC not exposed to any metal nanoparticles at each Co nanoparticles concentration tested ($p>0.05$). Generally, MSC exposed to titanium had higher elasticity than those treated with cobalt ($p<0.05$).

Spring constant (k_b) of MSCs not exposed to nanoparticles did not change with time ($p>0.05$). When MSCs were exposed to titanium nanoparticles for 24 hours (Figure 5), either the composition (elemental Ti or titanium oxide) or the concentrations had a significant effect compared to the control samples ($p<0.05$). Longer exposure time (48 and 72 hours) resulted in not significant alterations of the cell spring constant compared to control samples ($p>0.05$). Similar behaviour was recorded for cobalt nanoparticles (Figure 6); only after 24 hours of exposure Co 30 nm returning lower values of k_b at concentrations up to 12.5 $\mu\text{g}/\text{ml}$. Whilst Co 50 nm had a concentration dependent reduction of the cell elasticity. Also for Cobalt, longer exposure time (48 and 72 hours), did not result in significant alterations of the cell spring constant compared to control samples ($p>0.05$)

3.4 Metal uptake

Greater uptake was recorded with increasing concentration; increasing exposure time resulted in higher uptake for lower nanoparticles concentration (Figure 7). The composition of the particles seemed to be more important than the size as Ti 25 and 100 nm had similar uptakes while Ti 30 nm had generally lower metal uptake.

Similarly with Co, uptake increased with increasing concentration and over time again with the greatest uptake reached after 48 hours; additionally Co 50nm demonstrated the highest uptake at each time point and concentrations ($p<0.05$).

The main difference between the elements was that Co uptake was about an order of magnitude higher than Titanium.

3.5 Cell adhesion forces

Generally, MSC exposed either to both types of Co and Ti nanoparticles or not exposed to any nanoparticles exhibited a spatial distribution of the adhesion forces on the cell surface that did not follow a Gaussian distribution (Figure 8). No variation in the adhesion forces was detected for the control samples with increasing time; the median was in all three cases about 0.9 nN.

Ti nanoparticles generally did not cause variation in the adhesion forces of MSCs for exposure up to 2 days regardless of the size and composition (Figure 8) as the distributions of forces were not significantly different from the respective control. Instead, after 3 days of exposure to any of the Ti nanoparticles tested, MSCs exhibited smaller adhesion forces than MSCs that were not exposed to Ti nanoparticles even at the lowest concentration used in this work.

For cobalt nanoparticles (Figure 8) after 24 hours exposure there was not much difference in the lower quartiles, however, there was a general decrease in mean adhesion values with increasing concentration with the lowest value at 25 $\mu\text{g}/\text{ml}$ for both Co 30nm and Co 50nm. Furthermore, the distribution of adhesion forces was narrower for the two greatest concentration of nanoparticles tested. After 48 hours, the range of adhesion decreased for the control but the median remained almost unchanged. Largely, there was a decrease in overall adhesion with increasing concentration similarly to that at 24 hours. However, Co 50nm increased in adhesion at 50 $\mu\text{g}/\text{ml}$; and unlike 24 hours, Co 50nm had a smaller range of adhesion compared to Co 30nm except for the highest concentration. MSCs exposed for 72 hours a similar pattern was observed for the overall adhesion forces that as the concentration of nanoparticles increased the adhesion decreased.

4 Discussion

MSCs in trabecular bone [24] and adjacent to implants have osteoprogenitor activities and are critical contributors to maintaining osseous tissue integrity. Perturbation of MSC osteogenic activity may thus affect bony ingrowth and interface stability, leading to increased risk of loosening. It has been observed that exposure to metal wear particles results in reduced osteogenic differentiation and proliferation, and enhanced apoptosis in

human MSCs [18]-[19]. Arthroplasty devices can be made from ceramic, metal or plastic materials. Titanium, cobalt and their oxides are the common materials used, the size, composition and concentration range of the wear particles resulting from these devices have been determined from retrieval studies and found to be around 50 nm for Co and up to few hundreds nanometers for Ti [36]; therefore the particles used in this study are a good model to study the effect of wear debris produced by joint replacement devices.

The results of the MTT assay, that is based on cellular oxido-reductase enzyme activity, revealed that MSC exposed to nanoparticles had a lower activity (Figure 1); however, this did not result from the presence of structurally damaged/non-viable cells as demonstrated by the flow-cytometry data (Figure 2). On the other hand, epifluorescent microscopy showed the morphology of the cells to be altered (bleeping) (Figure 3), these alternations are likely linked with the changes in the mechanical properties measured using AFM (Figure 5 and Figure 6). The metal nanoparticles used in this study had a similar effect on metabolic activity of mouse osteoblast cells [27]. Nonetheless, in osteoblast cells reduced metabolic activity was still recorded after 3 days of exposure to nanoparticles while in the MSC employed in this work did not exhibit this as effects were detected only after in the first two days of exposure (Figure 1).

It has been recognised that the cell's mechanical properties have a role in the fate of the cell and affect a number of cell functions such as its differentiation [37],[38], ageing and diseased state [39],[40]. The structural integrity and the mechanical behaviour of cells are mainly controlled by the cell cytoskeleton and actin filaments organisation. This is the first time that AFM nanoindentation was applied to the investigation of the responses of MSCs to metal wear particles to identify the role of parameters such as particles size and composition and concentration; usually such investigations are limited to the determination of cytokine production, DNA damage or gene expression. Titushkin et al. (2006) [41] studied the membrane properties of mesenchymal stem cells and observed that normal cells had a spring constant anywhere between 0.001-0.1 N/m [41], this correlates well with the values measured in our study using the AFM for all control cells [42],[43]. Such variations can also be attributed to different fitting procedures; we modelled only the initial part of the indentation curve with the Hertz model as it is valid only for small indentation depths (up to about 200 nm). This is a consequence of the fact that it was formulated with the assumption

is of semi-infinite material; in order to operate when this assumption is still valid, an indentation depth of no more than 5-10% of the average cell height was suggested [44]. At greater indentation depths, a well-known linear relation between indentation depth and force was found and the slope of such relation determined (spring constant). The values of cell elasticity found here are slightly higher than in other works [44],[45], where few kPa, were found; this could be a consequence of the different type of cells and growing conditions; however, in some of these works [46] the full indentation curve was modelled with the Hertz model. The shape of the indentation curve (Figure 4) suggested that smaller Young moduli would be calculated in case the deeper part of the indentation curve was also included in the fitting algorithm.

Endocytosis of titanium or cobalt particles has been suggested as possible mode of wear particles action on MSCs [47],[48]. Cytoskeletal disruption is thus a likely cause of the inhibition of cellular functions, although the exact mechanisms remain to be analysed [19]. These hypothesis support our results showing that particles entered MSC (Figure 7) inducing biological (Figure 1) and structural and morphological responses (Figure 3, Figure 5 and Figure 6) but not complete cell damage (Figure 2) leading to non-viability. Our study clearly demonstrated that cells exposed to cobalt nanoparticles are affected more than titanium nanoparticles; furthermore, the concentration of the nanoparticles was a predominant factor other than size. For titanium nanoparticles, our combined results showing unaffected viability and mechanical properties are in agreement with Mao et al. 2015 [49]. Furthermore, the decrease of metabolic activity (Figure 1) of MSCs with longer exposure times was not linked to an increased cell death (Figure 2) for both cobalt and titanium nanoparticles. Interestingly, the greatest differences in MSC mechanical properties exposed to cobalt nanoparticles compared to control samples occurred in the first 24 hours (Figure 6); with further exposure the effect of the nanoparticles appeared to decrease and after 3 days of exposure the effect of the nanoparticles was not significant, this is in line with the uptake reaching a plateau after 48 hours of exposure (Figure 7). The distributions of both cell elasticity and spring constant did not exhibit a bimodal behaviour highlighting the homogeneity of MSCs response and is also correlated to the lack of dead cells, who exhibit different mechanical properties (data not shown) among the MSC population.

Cell spring constant is linked to turgidity, therefore it was expected to notice alteration in both parameters when MSC were exposed to nanoparticles. It has been noted that the elasticity of cells can only be stretched by 2-4% before the membrane ruptures [41],[48]; therefore, a reduction in cell elasticity must be coupled with a reduction in turgidity in order to minimise the cell volume variation. Our results (Figure 5 and Figure 6) exhibited the anticipated trend that was also reported by Preedy et al. 2015 [27] for osteoblast cells.

Adhesion forces originate from interfacial interactions between contacting bodies [50]. Our results generally depicted a trend of reduction of adhesion force when exposed to nanoparticles, particularly for cobalt (Figure 8). This suggests that the nanoparticles can interfere with stem cell proliferation through preventing or weakening adhesion to a substrate that is the first step into stem cell growth.

Our results hint that the lower impact of titanium nanoparticles on MSC mechanical properties than cobalt nanoparticles is linked to a lower cell uptake of the former than the later (Figure 7). In addition, they support the general knowledge of titanium being more biocompatible than cobalt [20].

5 References

- [1] Tee, S.-Y., J. Fu, Christopher s. Chen, and Paul a. Janmey, Cell Shape and Substrate Rigidity Both Regulate Cell Stiffness. *Biophysical Journal*, 2011;100(5):L25-L27.
- [2] Tee, S.-Y., A.R. Bausch, and P.A. Janmey, The mechanical cell. *Current Biology*, 2009;19(17): R745-R748.
- [3] Guo, Q., Y. Xia, M. Sandig, and J. Yang, Characterization of cell elasticity correlated with cell morphology by atomic force microscope. *Journal of Biomechanics*, 2012;45(2):304-309.
- [4] Cai, P., Y. Mizutani, M. Tsuchiya, John m. Maloney, B. Fabry, Krystyn j. Van vliet, and T. Okajima, Quantifying Cell-to-Cell Variation in Power-Law Rheology. *Biophysical Journal*, 2013;105(5):1093-1102.
- [5] Bahraminasab, M., B.B. Sahari, K.L. Edwards, F. Farahmand, M. Arumugam, and T.S. Hong, Aseptic loosening of femoral components – A review of current and future trends in materials used. *Materials & Design*, 2012;42(0):459-470.
- [6] Kowandy, C., H. Mazouz, and C. Richard, Isolation and analysis of articular joints wear debris generated in vitro. *Wear*, 2006;261(9):966-970.

- [7] Prokopovich, P., S. Perni, J. Fisher, and R.M. Hall, Spatial variation of wear on Charité lumbar discs. *Acta Biomaterialia*, 2011;7(11):3914-3926.
- [8] Ingham, E. and J. Fisher, The role of macrophages in osteolysis of total joint replacement. *Biomaterials*, 2005;26(11):1271-1286.
- [9] Abu-Amer, Y., I. Darwech, and J.C. Clohisy, Aseptic loosening of total joint replacements: mechanisms underlying osteolysis and potential therapies. *Arthritis Research & Therapy*, 2007;9(Suppl 1):S6-S6.
- [10] Tuan, R.S., F.Y. Lee, T.K. Y, J.M. Wilkinson, and R.L. Smith, What are the local and systemic biologic reactions and mediators to wear debris, and what host factors determine or modulate the biologic response to wear particles? *J Am Acad Orthop Surg*, 2008;16 Suppl 1: S42-48.
- [11] Tella, S.H. and J.C. Gallagher, Prevention and treatment of postmenopausal osteoporosis. *The Journal of Steroid Biochemistry and Molecular Biology*, 2014;142(0):155-170.
- [12] Papageorgiou, I., C. Brown, R. Schins, S. Singh, R. Newson, S. Davis, J. Fisher, E. Ingham, and C.P. Case, The effect of nano- and micron-sized particles of cobalt–chromium alloy on human fibroblasts in vitro. *Biomaterials*, 2007;28(19):2946-2958.
- [13] Naudie, D.D., D.J. Ammeen, G.A. Engh, and C.H. Rorabeck, Wear and osteolysis around total knee arthroplasty. *J Am Acad Orthop Surg*, 2007;15(1):53-64.
- [14] Vermes, C., R. Chandrasekaran, J.J. Jacobs, J.O. Galante, K.A. Roebuck, and T.T. Glant, The effects of particulate wear debris, cytokines, and growth factors on the functions of MG-63 osteoblasts. *J Bone Joint Surg Am*, 2001;83-a(2):201-211.
- [15] Ingham, E. and J. Fisher, Biological reactions to wear debris in total joint replacement. *Proc Inst Mech Eng H*, 2000;214(1):21-37.
- [16] Behl, B., I. Papageorgiou, C. Brown, R. Hall, J.L. Tipper, J. Fisher, and E. Ingham, Biological effects of cobalt-chromium nanoparticles and ions on dural fibroblasts and dural epithelial cells. *Biomaterials*, 2013;34(14):3547-3558.
- [17] Papageorgiou, I., R. Marsh, J.L. Tipper, R.M. Hall, J. Fisher, and E. Ingham, Interaction of micron and nano-sized particles with cells of the dura mater. *Journal of Biomedical Materials Research - Part B Applied Biomaterials*, 2014;102(7):1496-505
- [18] Wang, M.L., L.J. Nesti, R. Tuli, J. Lazatin, K.G. Danielson, P.F. Sharkey, and R.S. Tuan, Titanium particles suppress expression of osteoblastic phenotype in human mesenchymal stem cells. *Journal of Orthopaedic Research*, 2002;20(6):1175-1184.
- [19] Okafor, C.C., H. Haleem-Smith, P. Laqueriere, P.A. Manner, and R.S. Tuan, Particulate endocytosis mediates biological responses of human mesenchymal stem cells to titanium wear debris. *Journal of Orthopaedic Research*, 2006;24(3):461-473.
- [20] Schofer, M.D., S. Fuchs-Winkelmann, A. Kessler-Thones, M.M. Rudisile, C. Wack, J.R. Paletta, and U. Boudriot, The role of mesenchymal stem cells in the pathogenesis of Co-Cr-Mo particle induced aseptic loosening: an in vitro study. *Biomed Mater Eng*, 2008;18(6):395-403.
- [21] Chiu, R., T. Ma, R.L. Smith, and S.B. Goodman, Kinetics of polymethylmethacrylate particle-induced inhibition of osteoprogenitor differentiation and proliferation. *Journal of Orthopaedic Research*, 2007;25(4):450-457.

- [22] Chiu, R., K.E. Smith, G.K. Ma, T. Ma, R.L. Smith, and S.B. Goodman, Polymethylmethacrylate particles impair osteoprogenitor viability and expression of osteogenic transcription factors Runx2, osterix, and Dlx5. *Journal of Orthopaedic Research*, 2010;28(5):571-577.
- [23] Song, L., N.J. Young, N.E. Webb, and R.S. Tuan, Origin and characterization of multipotential mesenchymal stem cells derived from adult human trabecular bone. *Stem Cells Dev*, 2005;14(6):712-721.
- [24] Nöth, U., A.M. Osyczka, R. Tuli, N.J. Hickok, K.G. Danielson, and R.S. Tuan, Multilineage mesenchymal differentiation potential of human trabecular bone-derived cells. *Journal of Orthopaedic Research*, 2002;20(5):1060-1069.
- [25] Weissleder, R., M. Nahrendorf, and M.J. Pittet, Imaging macrophages with nanoparticles. *Nat. Mater*, 2014;13(2):125-138.
- [26] E. Callard Preedy, S. Perni, P. Prokopovich, Nanomechanical and Surface Properties of rMSCs post Exposure to CAP Treated UHMWPE Wear Particles. *Nanomed.: Nanotech. Biol. Med.* doi:10.1016/j.nano.2015.10.006
- [27] E. Callard Preedy, S. Perni, P. Prokopovich, Cobalt, Titanium and PMMA Bone Cement Debris Influence on Mouse Osteoblasts Cell Elasticity, Spring constant and Calcium Production Activity. *RSC Advances* 2015;5:83885-83898.
- [28] Helenius, J., C.P. Heisenberg, H.E. Gaub, and D.J. Muller, Single-cell force spectroscopy. *J Cell Sci*, 2008;121(Pt 11):1785-1791.
- [29] Yang, R., N. Xi, K.W.C. Lai, K. Patterson, H. Chen, B. Song, C. Qu, B. Zhong, and D.H. Wang, Cellular biophysical dynamics and ion channel activities detected by AFM-based nanorobotic manipulator in insulinoma β -cells. *Nanomedicine : nanotechnology, biology, and medicine*, 2013;9(5): 636-645.
- [30] Xu, W., R. Mezencev, B. Kim, L. Wang, J. McDonald, and T. Sulchek, Cell Stiffness Is a Biomarker of the Metastatic Potential of Ovarian Cancer Cells. *PLoS ONE*, 2012;7(10):e46609.
- [31] Phinney, D.G., G. Kopen, R.L. Isaacson, and D.J. Prockop, Plastic adherent stromal cells from the bone marrow of commonly used strains of inbred mice: variations in yield, growth, and differentiation. *J Cell Biochem*, 1999;72(4):570-585.
- [32] Harrington, J., A.J. Sloan, and R.J. Waddington, Quantification of clonal heterogeneity of mesenchymal progenitor cells in dental pulp and bone marrow. *Connect Tissue Res*, 2014;55 Suppl 1:62-67.
- [33] Preedy, E.C., E. Brousseau, S. Evans, S. Perni, and P. Prokopovich, Adhesive Forces and Surface Properties of Cold Gas Plasma Treated UHMWPE. *Colloids and Surfaces B: Biointerfaces*, 2014;460:83-89.
- [34] Sader, J.E., J.A. Sanelli, B.D. Adamson, J.P. Monty, X. Wei, S.A. Crawford, J.R. Friend, I. Marusic, P. Mulvaney, and E.J. Bieske, Spring constant calibration of atomic force microscope cantilevers of arbitrary shape. *Review of Scientific Instruments*, 2012;83(10):103705-103705-16.
- [35] Sader, J.E., I. Larson, P. Mulvaney, and L.R. White, Method for the calibration of atomic force microscope cantilevers. *Review of Scientific Instruments*, 1995;66(7):3789-3798.

- [36] Prokopovich, P., Interactions between mammalian cells and nano- or micro-sized wear particles: Physico-chemical views against biological approaches. *Advances in Colloid and Interface Science*, 2014;213(0):36-47.
- [37] Docheva, D., D. Padula, C. Popov, W. Mutschler, H. Clausen-Schaumann, and M. Schieker, Researching into the cellular shape, volume and elasticity of mesenchymal stem cells, osteoblasts and osteosarcoma cells by atomic force microscopy. *Journal of Cellular and Molecular Medicine*, 2008;12(2):537-552
- [38] Settleman, J., Tension precedes commitment-even for a stem cell. *Mol Cell*, 2004;14(2):148-150.
- [39] Suresh, S., Biomechanics and biophysics of cancer cells. *Acta Biomaterialia*, 2007;3(4):413-438.
- [40] Jin, H., X. Xing, H. Zhao, Y. Chen, X. Huang, S. Ma, H. Ye, and J. Cai, Detection of erythrocytes influenced by aging and type 2 diabetes using atomic force microscope. *Biochemical and Biophysical Research Communications*, 2010;391(4):1698-1702.
- [41] Titushkin, I. M. Cho, Distinct membrane mechanical properties of human mesenchymal stem cells determined using laser optical tweezers. *Biophys J*, 2006;90(7):2582-2591.
- [42] Titushkin, I. M. Cho, Altered osteogenic commitment of human mesenchymal stem cells by ERM protein-dependent modulation of cellular biomechanics. *Journal of Biomechanics*, 2011;44(15):2692-2698.
- [43] Simon, A., T. Cohen-Bouhacina, M.C. Porté, J.P. Aimé, J. Amédée, R. Bareille, C. Baquey, Characterization of dynamic cellular adhesion of osteoblasts using atomic force microscopy. *Cytometry Part A*, 2003;54A(1):36-47.
- [44] Titushkin, I. M. Cho, Modulation of cellular mechanics during osteogenic differentiation of human mesenchymal stem cells. *Biophys J*, 2007;93(10):3693-702.
- [45] Kuznetsova, T.G., M.N. Starodubtseva, N.I. Yegorenkov, S.A. Chizhik, R.I. Zhdanov, Atomic force microscopy probing of cell elasticity. *Micron*, 2007;38(8):824-833.
- [46] Haghi, M., D. Traini, L.G. Wood, B. Oliver, P.M. Young, W. Chrzanowski, A 'soft spot' for drug transport: modulation of cell stiffness using fatty acids and its impact on drug transport in lung model. *Journal of Materials Chemistry B*, 2015;3(13):2583-2589.
- [47] Schröck, K., H. Schneider, J. Lutz, M.C. Hacker, S. Mändl, M. Kamprad, M. Schulz-Siegmund, Cytocompatibility of nitrogen plasma ion immersed medical cobalt–chromium alloys. *Journal of Biomedical Materials Research Part A*, 2014;102(6):1744-1754.
- [48] Wang, Y., Q. Wu, K. Sui, X.X. Chen, J. Fang, X. Hu, M. Wu, and Y. Liu, A quantitative study of exocytosis of titanium dioxide nanoparticles from neural stem cells. *Nanoscale*, 2013;5(11):4737-4743.
- [49] Mao, Z., B. Xu, X. Ji, K. Zhou, X. Han, M. Chen, X. Zhang, Q. Tang, X. Wang, and Y. Xia, Titanium dioxide nanoparticles alter cellular morphology via disturbing their microtubule dynamics. *Nanoscale* 2015;7(18):8466-8475.
- [50] Perni, S., E.C. Preedy, and P. Prokopovich, Success and failure of colloidal approaches in adhesion of microorganisms to surfaces. *Advances in Colloid and Interface Science*, 2014;759 206(0):265-274.

6 Figures Captions

Figure 1. MTT results of MSCs exposed to Titanium nanoparticles for (a) 24h, (b) 48 h and (c) 72 h or exposed to Cobalt nanoparticles for (d) 24h, (e) 48 h and (f) 72 h.

□ Control ■ Ti 30 nm □ Ti 25 nm ■ Ti 100 nm ▨ Co 30 nm ▩ Co 50 nm

Figure 2. Viability of MSCs exposed to either Titanium nanoparticles for (a) 24h, (b) 48 h and (c) 72 h or to Cobalt nanoparticles for (d) 24h, (e) 48 h and (f) 72 h.

□ alive ■ injured ■ dead

Figure 3. Example of fluorescence images (x10 magnification) of MSCs after 24h without particles (control sample) stained with FDA (a) or PI (d) and MSCs exposed for 24h to either 50 µg/ml of Ti 30nm and stained with FDA (b) or PI (e) or Co 50 nm and stained with FDA (c) or PI (f). Bar represents 100 µm.

Figure 4. Examples of MSCs indentation curve for MSC not exposed to nanoparticles after 24h incubation (———).

——— Hertz model fitting - - - - Hooke model fitting.

Figure 5. Mean cell elasticity (right side) and spring constant (left side) of MSCs exposed to Titanium nanoparticles for (a, d) 24h, (b, e) 48 h and (c, f) 72 h.

□ Control ■ Ti 30 nm □ Ti 25 nm ■ Ti 100 nm

Figure 6. Mean cell elasticity (right side) and spring constant (left side) of MSCs exposed to Cobalt nanoparticles for (a, d) 24h, (b, e) 48 h and (c, f) 72 h.

□ Control ■ Co 30 nm □ Co 50 nm

Figure 7. Metal uptake of MSCs exposed to Titanium (a) Ti 25 nm, (b) Ti 30 nm, (c) Ti 100 nm, (d) Co 30 nm and (e) Co 50 nm at different concentrations.

24 h ■ 48 h □ 72h ■

Figure 8. Adhesion force distribution of MSC cells exposed to either Titanium or Cobalt nanoparticles for (a, d) 24h, (b, e) 48 h and (c, f) 72 h.

□ control ■ Ti 25 nm ▨ Ti 30 nm ■ Ti 100 nm ▩ Co 30 nm ▩ Co 50 nm

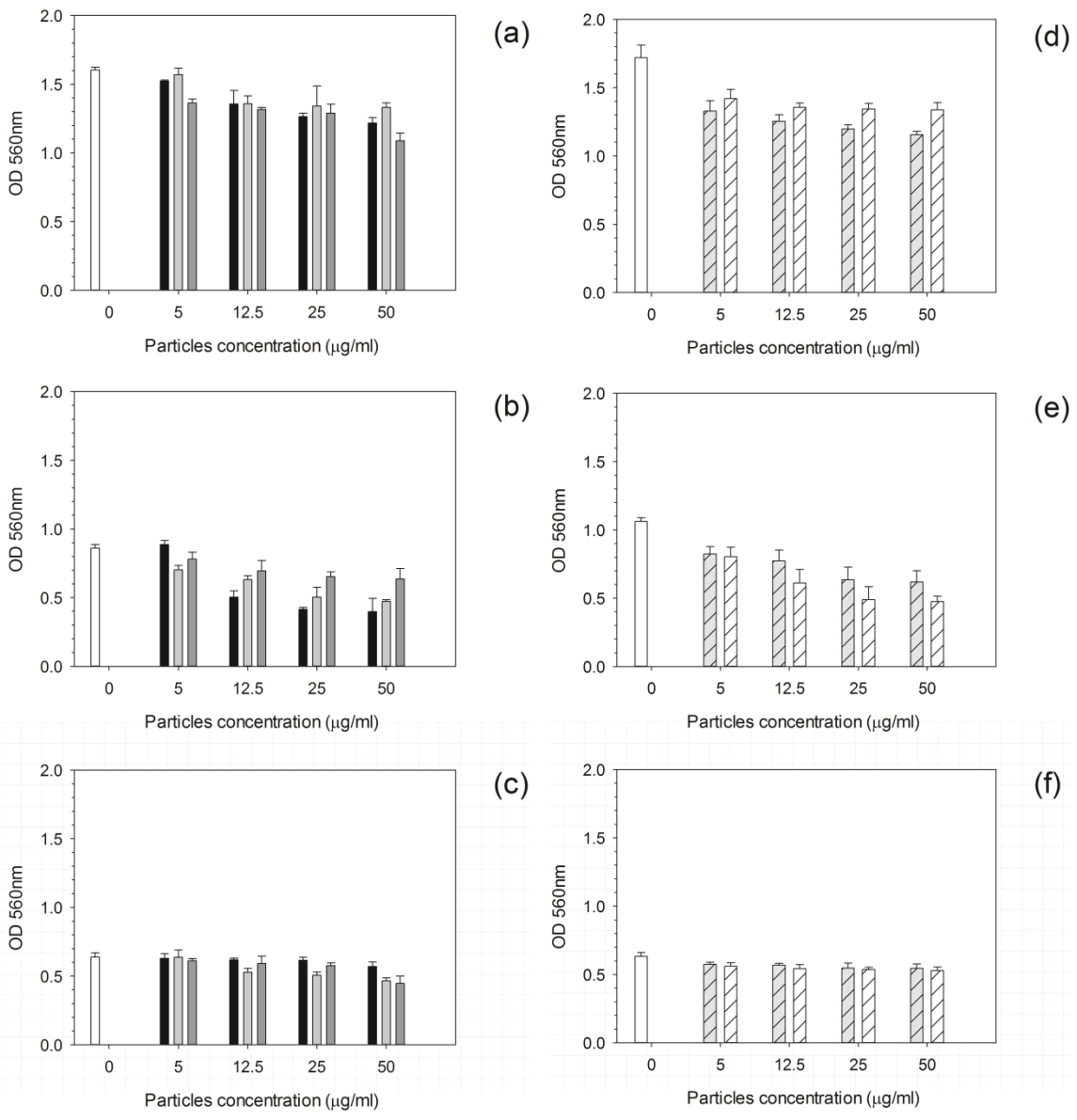


Figure 1

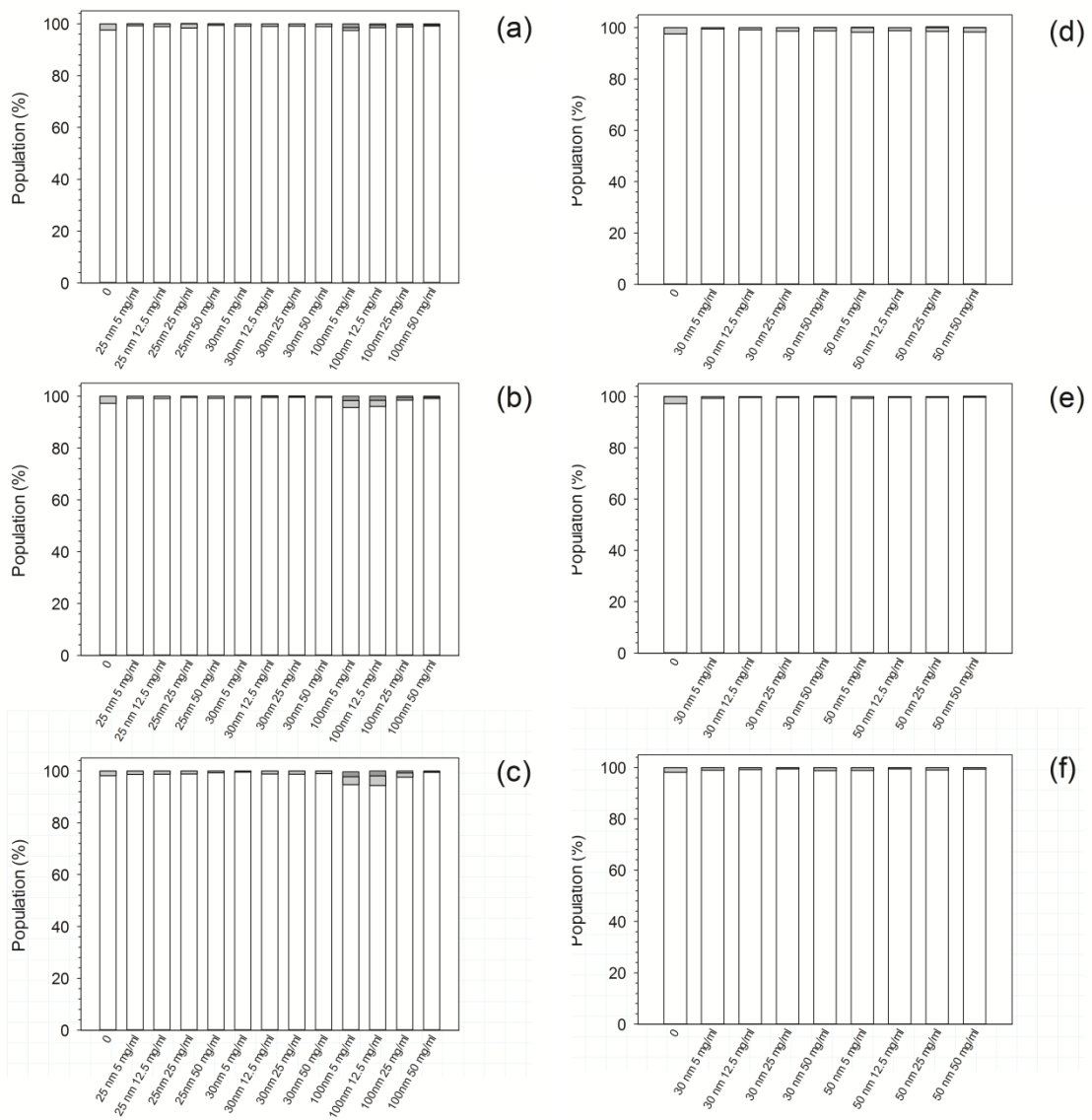


Figure 2

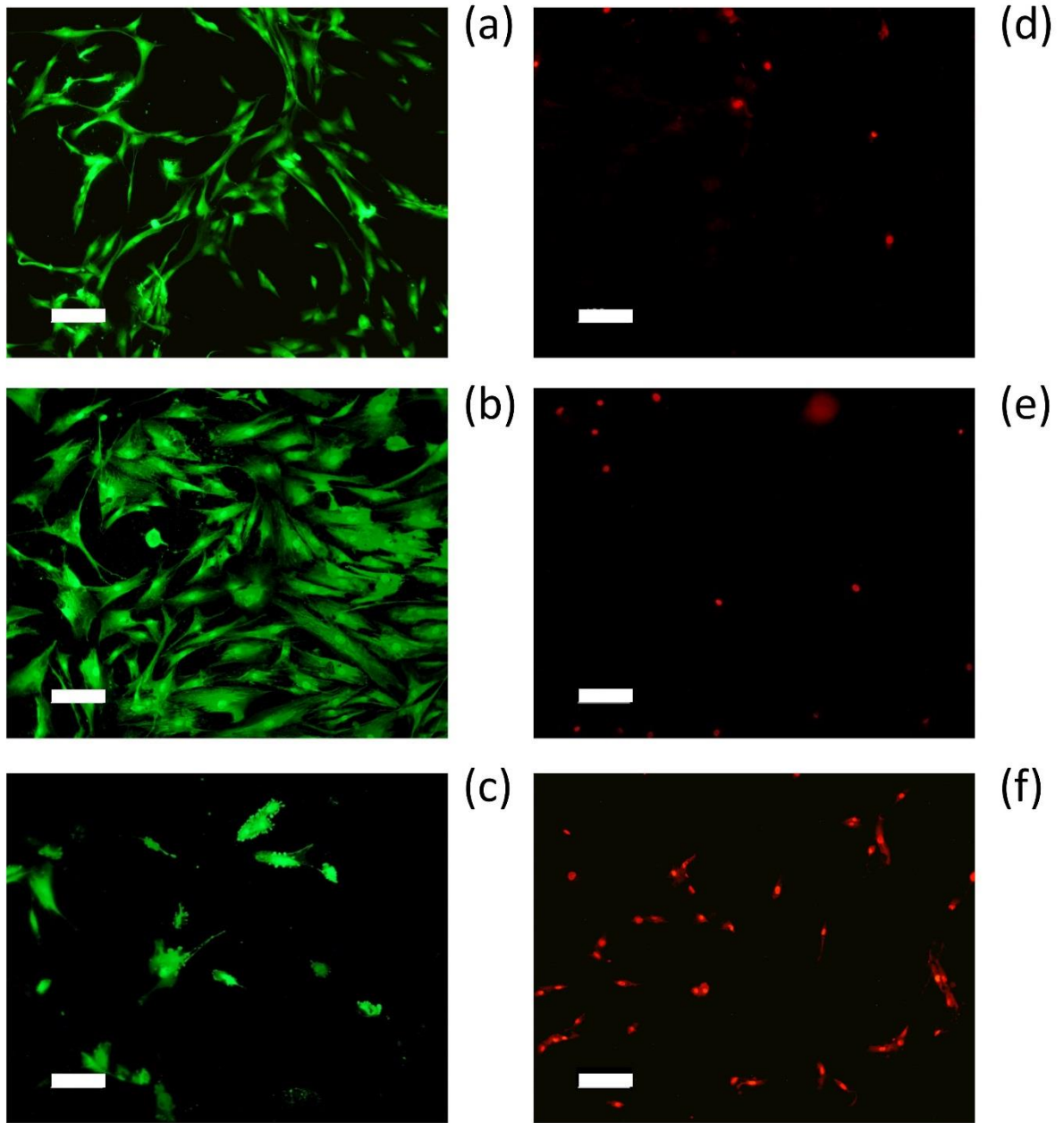


Figure 3

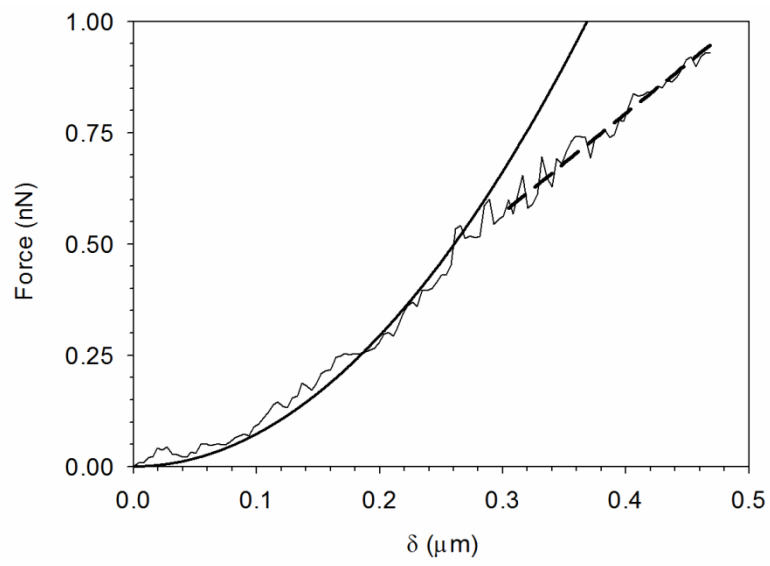


Figure 4

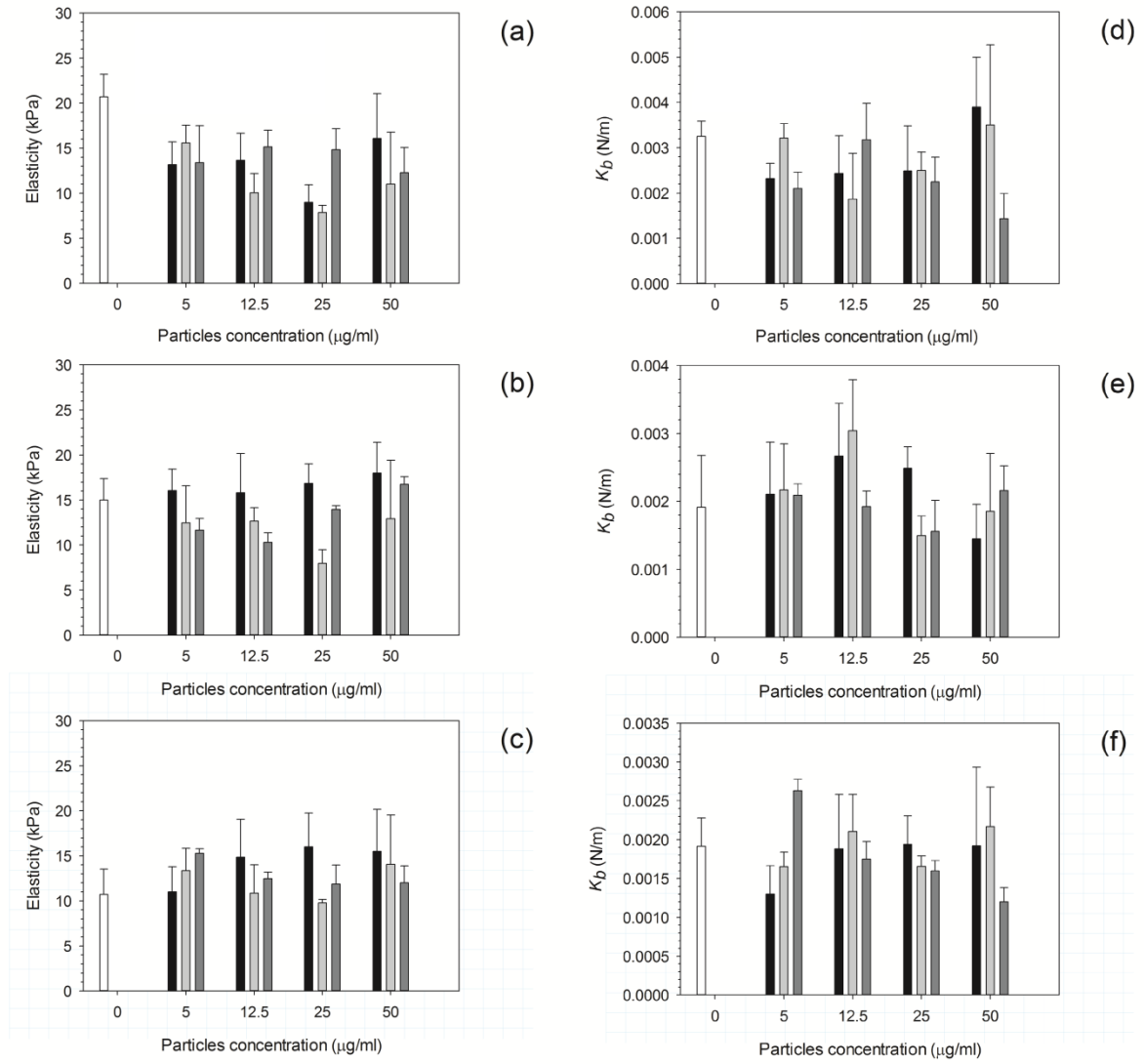


Figure 5

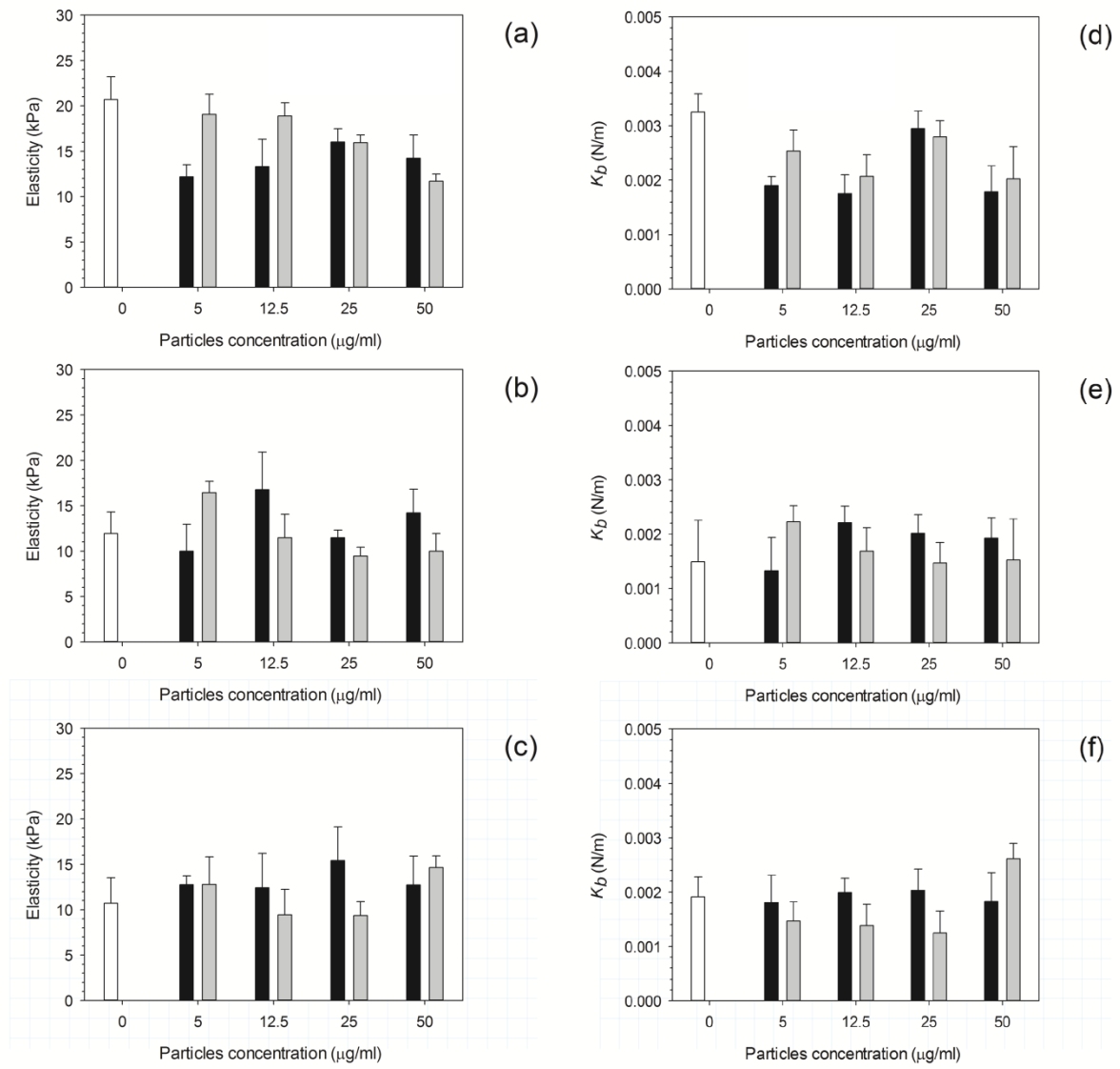


Figure 6

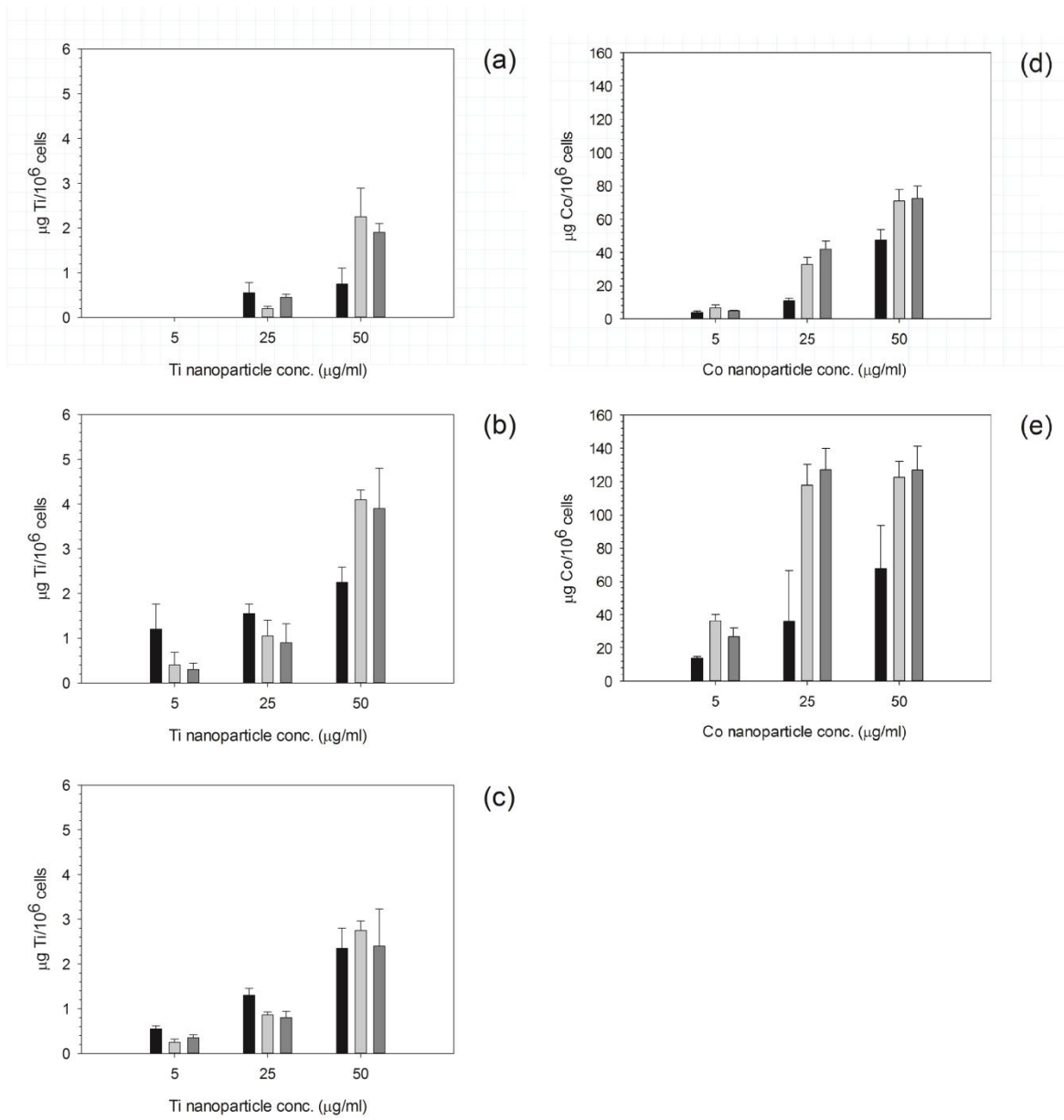


Figure 7

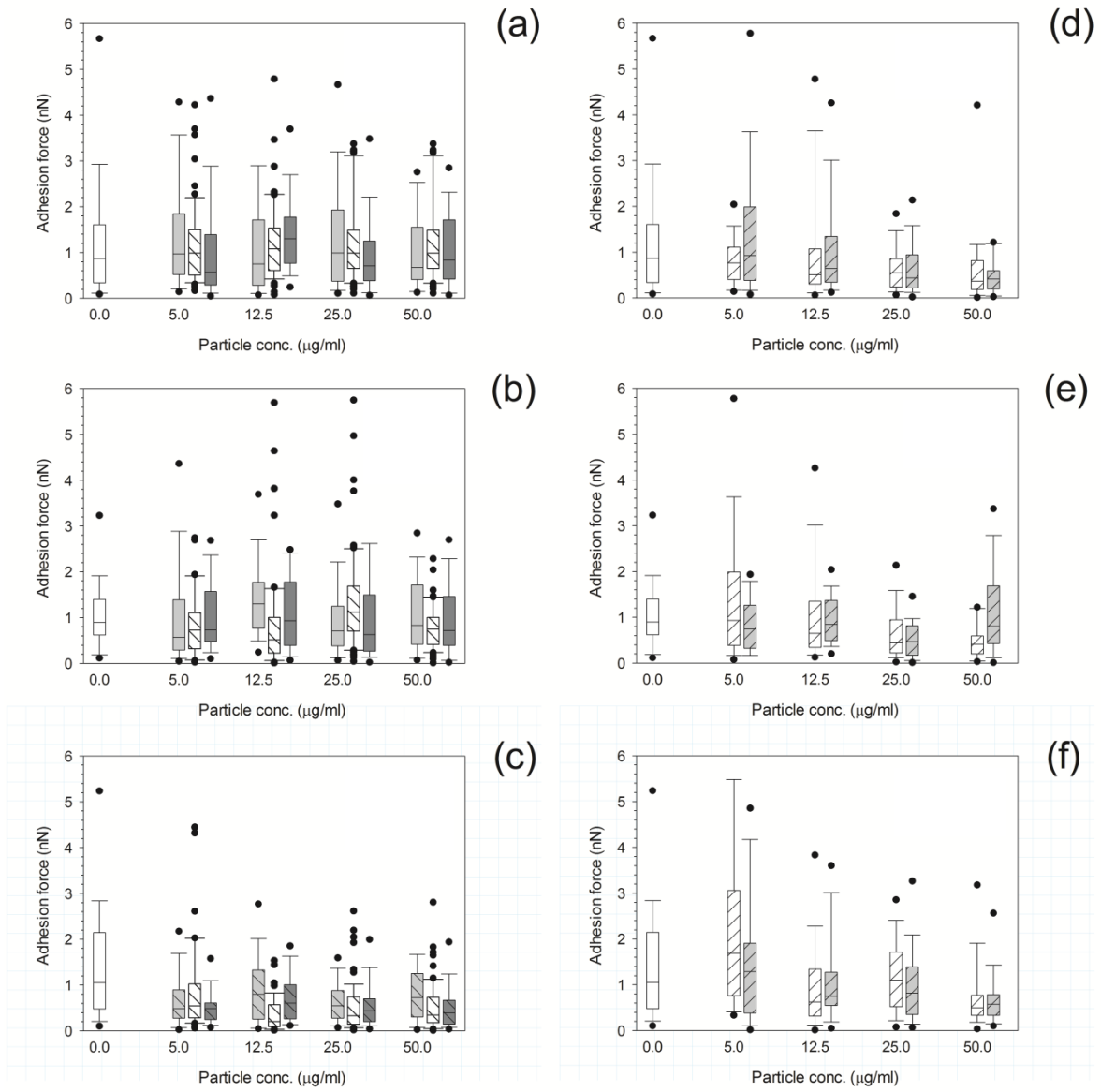


Figure 8